InAs/GaSb Superlattice Photodiodes Operating in the Midwave Infrared Range

P. Christol[1], R. Taalat[1], C. Cervera[1], H. Aït-Kaci[1], M. Delmas[1], J. B. Rodriguez[1], E. Giard[2] and I. Ribet-Mohamed[2]
[1]*Institut d'Electronique du Sud, UMR-CNRS 5214, Université Montpellier 2, Place Eugène Bataillon, 34095 Montpellier Cedex 5, France*
[2]*ONERA, Chemin de la Hunière, 91761 Palaiseau, France*

Keywords: Photodiode, Midwave Infrared, InAs/GaSb Superlattice.

Abstract: This communication reports on InAs/GaSb superlattice (SL) pin photodiodes. The SL structures, fabricated by molecular beam epitaxy (MBE), are made of symmetrical and asymmetrical period designs adapted for the Midwave Infrared (MWIR) domain, with cut-off wavelength near 5µm at 77K. The structures are studied in terms of dark current-voltage measurements. Comparison of results revealed the predominance of the asymmetric SL design with dark current densities $J = 4x10^{-8}A/cm^2$ at 77K for V_{bias} = -50mV and R_0A product equal to $1.5x10^6\Omega.cm^2$ at 77K, one order of magnitude higher than the symmetric SL structures. Such result demonstrates the strong influence of the period on the electrical properties of SL MWIR photodiodes.

1 INTRODUCTION

Infrared (IR) photodetectors based on type-II InAs/GaSb superlattice (SL) material has been given a lot of attention this past decade. Among the advantages of this material system, one can cite the possibility to span a large IR range (3 to 30 µm) by tailoring the band-gap independently from the lattice constant, allowing addressing many applications by the same fabrication process and the realization of multi-color IR sensors for high performance imaging systems.

Since the first works of Yang and Bennet in 1994 (Yang et al., 1994), impressive progresses were obtained on MWIR SL detectors. Indeed, the maturity of the growth of the SL quantum structure by molecular beam epitaxy (MBE) (Kaspi et al., 2001); (Haugan et al., 2004); (Satpati et al.,, 2007) and progress on the processing of SL devices (Hood et al., 2007); (Chaghi et al.,, 2009); (Plis et al., 2011) resulted in the demonstration of high-performance mega-pixel focal plane arrays (FPA) in midwave infrared (MWIR) spectral bands (Rehm et al., 2006); (Little et al., 2007); (Gunapala et al., 2010); (Abdollahi et al., 2011). Consequently, InAs/GaSb SL detector can be now considered as a complementary technology to the well-established InSb and HgCdTe MWIR photodiodes (Rogalski et al., 2009).

Reported SL periods for MWIR operation usually comprise GaSb and InAs layer thicknesses in the range of 8 to 11 monolayers (MLs), and most of the SL periods reported are symmetric with an InAs to GaSb thickness ratio close to one (Rodriguez et al., 2005); (Cervera et al.,, 2009); (Rehm et al., 2006); (Little et al., 2007); (Wei et al., 2005); (Hill et al., 2007). The period composition affects many material characteristics such as the effective masses and therefore the intrinsic carrier concentration, involved in both the diffusion (J_{diff}) and generation-recombination (J_{GR}) dark-currents. It also affects the electron-holes wave-function overlap which is involved in the external quantum efficiency of the device. Consequently, it is clear that the SL period composition has implications on both the signal and the noise of the photodetector. Its optimization should lead to improve device performances or temperature operation.

In this paper, we report on dark current-voltage measurements of MWIR pin SL photodiodes grown by molecular beam epitaxy (MBE) on p-type GaSb substrates. Two designs of SL period were fabricated with a 5µm cut-off wavelength at 77K. A

Christol P., Taalat R., Cervera C., Aït-Kaci H., Delmas M., Rodriguez J., Giard E. and Ribet-Mohamed I..
InAs/GaSb Superlattice Photodiodes Operating in the Midwave Infrared Range.
DOI: 10.5220/0004222600910095
In *Proceedings of the International Conference on Photonics, Optics and Laser Technology* (PHOTOPTICS-2013), pages 91-95
ISBN: 978-989-8565-44-0

symmetric SL period made of 10 InAs MLs and 10 GaSb MLs (10/10 SL) and an asymmetric period design, with an InAs to GaSb thickness ratio close to 2, made of 7 InAs MLs and 4 GaSb MLs (7/4 SL). Comparison of results obtained showed the influence of the SL period design on the electrical performances of the SL MWIR photodiodes.

2 PHOTODIODES FABRICATION

The samples were grown in a Varian Gen II MBE reactor equipped with tellurium and beryllium dopant cells, and valved cracker cells for both arsenic and antimony. The pin SL structures (Figure 1) were grown on two inch (2") GaSb (100) wafers, p-type doped in the 5-8x10^{17}/cm^3 range, mounted on an In-free molybdenum holder. The pin device consisted of a 500 nm thick Be-doped (p = 1x10^{18} /cm^3) GaSb contact layer, followed by a non-intentionally doped (nid) absorbing layer of 1µm of 10 MLs InAs/10 MLs GaSb (10/10) symmetric (170 periods) or 7MLs InAs/4MLs GaSb (7/4) asymmetric (310 periods) MLs SL design and capped with a 100nm or 20 nm thick InAs Te-doped (n = 1x10^{18} /cm^3) top contact layer. The first and last 10 SL periods are p and n-type doped respectively to decrease the energy band offsets existing with the GaSb and InAs contact layers.

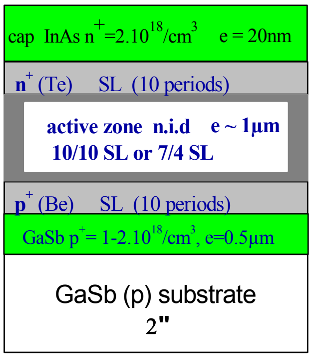

Figure 1: Schematic diagram of the InAs/GaSb pin SL MWIR structures on p-type GaSb. The SL active zone is composed of 10/10 symmetric or 7/4 asymmetric period design, for a total thickness of 1µm.

Structural characterizations were routinely performed on the SL samples. According to X-ray diffractometry data, SL structures lattice matched to the GaSb substrate were obtained. An example of high resolution X-ray diffraction spectrum of a perfectly matched SL structure on the GaSb substrate is shown on Figure 2.

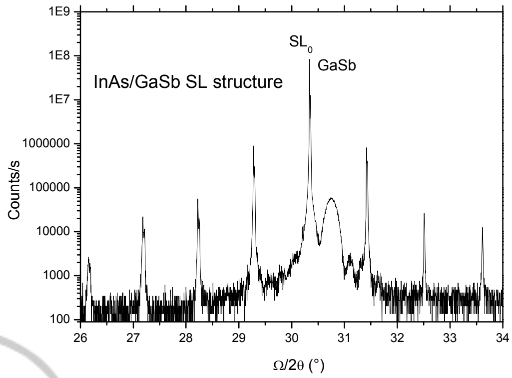

Figure 2: HRXRD patterns of 170 periods InAs/GaSb 10/10 SL structures lattice-matched to the GaSb substrate.

Concerning optical characterizations, the 10/10 and 7/4 SL structures exhibited photoluminescence (PL) spectra at 80K at 5µm (Figure 3).

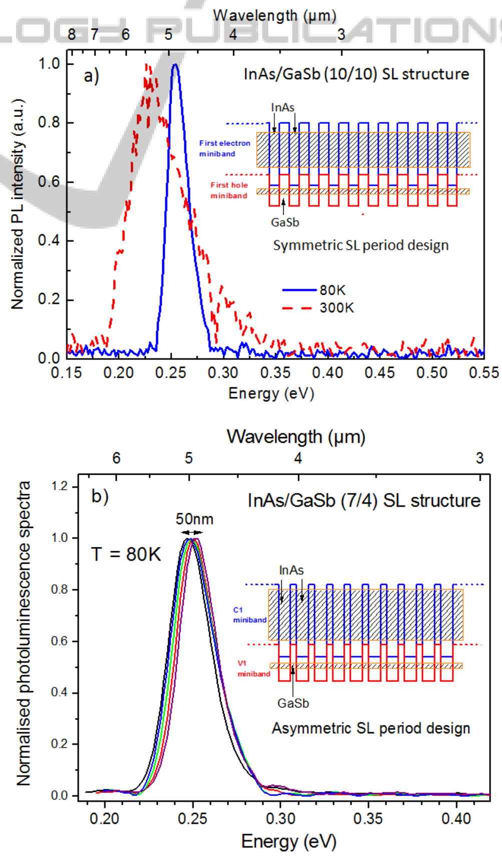

Figure 3: Normalized photoluminescence spectra of symmetric 10/10 (a) and asymmetric 7/4 (b) SL structures. In inset, band diagram of the SL structure showing first electron C1 and hole V1 minibands.

In particular, a set of several 7/4 SL samples with active layer thicknesses varying from 1µm (310 periods) to 4µm (1240 periods) have been grown, exhibiting photoluminescence emission at around 5µm at 77K (Figure 3b). This result shows the reproducibility and the control of the MBE grown SL structures.

From epitaxial SL material, circular mesa photodiodes were fabricated using standard photolithography with a mask set containing diodes and photodiodes with several diameters, from 60µm up to 310µm (inset of Figure 4). Metallization were ensured by CrAu sputtering on the p-GaSb substrate and on the n-type InAs cap layer. Mesa photodiodes were realized by wet etching using H_3PO_4 / H_2O_2 / $H_2O/C_6H_8O_7$ solution followed by NaClO smoothing (Chaghi et al.,, 2009).

To complete the device processing, photoresist AZ-1518 was spun onto the sample in order to protect the surface from ambient air. Then, the same mask as the one used for front-side metallization was used to open paths for wire bonding and the photoresist was heated at 200°C for 2 hours to be polymerized.

Finally, the samples were wire bounded and packaged in TO-8 sub-mounts. The devices were placed in a liquid nitrogen cryostat in order to perform characterizations at low temperature. Illuminating the device frontside, the spectral response of the unbiased photodiode was measured using a FTIR spectrometer. The asymmetric 7/4 SL photodetector exhibits cut-off wavelength at around 5µm at 80K (Figure 4), consistent with the PL peak positions presented in Figure 3b.

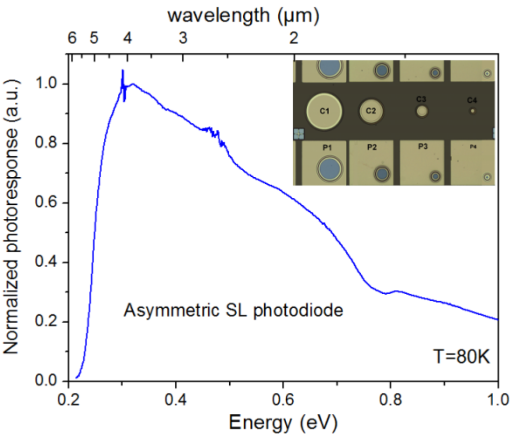

Figure 4: Photoresponse spectrum of InAs/GaSb (7/4) SL photodiode at 80K. In inset, top view of a processed sample, diodes (C) and photodiodes (P) with several diameters from 60µm up to 310µm.

3 PHOTODIODES ELECTRICAL CHARACTERIZATION

In order to perform current-voltage (I-V) characterization in dark conditions, a KEITHLEY 6417A Electrometer was used to both apply the bias voltage and read the current delivered by the SL device. Figures 5a and 5b show J-V curves at 77K of the pin symmetric 10/10 and asymmetric 7/4 SL diodes, respectively, for a bias voltage in the range [-1V, +0.3V]. Whatever the diode, no leakage currents in volume at reverse bias or no surface leakage currents in forward bias are observed. Extracted from J(V) curves, dynamic resistance–area products R_dA are also plotted in Figure 5. At V=0V, the R_0A product is one of the figures of merit of IR photodiodes (Rogalski et al., 2009).

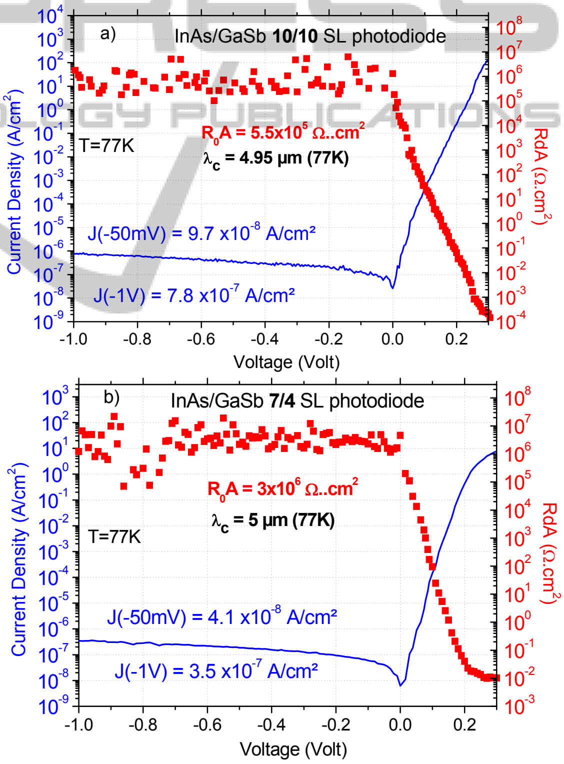

Figure 5: Dark current density measurements J(V) at 77K performed on symmetric 10/10 (a) and asymmetric 7/4 (b) SL pin photodiodes. The dynamic resistance area products R_dA as a function of bias are extracted from J(V) curves.

For the symmetric 10/10 SL device having cut-off at 4.95µm, results at 77K show dark current density at V=-50mV inferior to $1x10^{-7}$ A/cm^2 and a R_0A product superior to $5x10^5$ Ω.cm^2 (Figure 5a).

For the asymmetric 7/4 SL diodes, results show an increase of performances with J(-50mV) = 4.1x10^{-8} A/cm^2 and R_0A as high as 3.5x10^6 Ω.cm^2 , which is one of the best R_0A value reported for a diode having a cut-off wavelength at 5µm at 77K.

Figure 6 displays J(V) curves of the asymmetric 7/4 SL diode for different temperatures ranging from 77K to 300K. At room temperature, J (-50mV) = 10 A/cm^2 was measured and a good R_0A value of 1x10^{-2} Ω.cm² was deduced from this measurement.

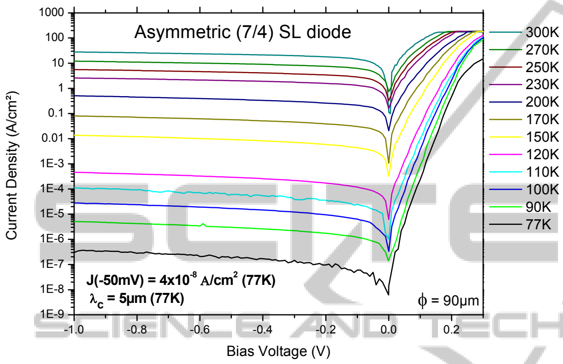

Figure 6: Asymmetric 7/4 SL pin photodiode : Dark current density-voltage characteristics for different operating temperature [77-300K].

Extracted from J-V measurements, dark current densities at 50mV reverse bias are reported as a function of inverse temperature (Arrhenius plot) in Figure 7. Temperature dependence of the dark-current density reveals that the 7/4 SL device is diffusion-limited at high temperature, while it is GR-limited below 120K.

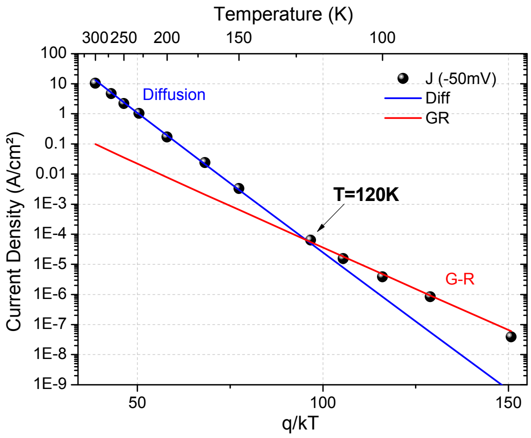

Figure 7: Asymmetric 7/4 SL pin photodiode : Arrhenius plot of the dark current density (-50mV). The diffusion and GR limited regimes are reported.

4 PHOTODIODES COMPARISON

For several symmetric and asymmetric photodiodes operating in the MWIR domain, the results obtained, in terms of R_0A, are compared in Figures 8. Significant results extracted from literature (Rehm et al., 2006); (Wei et al., 2005); (Walther et al., 2006); (Hill et al., 2007) have also been reported.

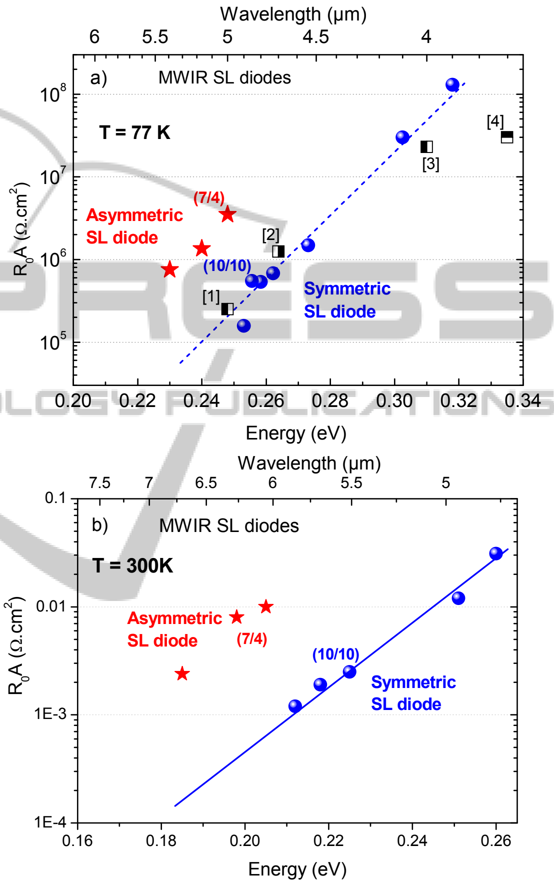

Figure 8: Experimental values of R_0A product versus cut-off wavelength for both symmetric (circle) and asymmetric (star) MWIR SL structures at 77K (a) and 300K (b), and comparison (square) with typical results of SL pin diodes extracted from literature (1-Rhem et al., 2006; 2-Wei et al., 2005; 3-Walther et al., 2006; 4-Hill et al., 2007).

Figure 8a (77K) and Figure 8b (300K) show that, whatever the temperature, at low temperature when the InAs/GaSb SL diode is GR limited or at high temperature when the SL diode is diffusion limited, the R_0A values of the asymmetrical SL photodiodes are always, at least, one decade higher than the symmetrical SL design. This improvement of R_0A values for the asymmetric SL is due to the reduction of GaSb layer in the InAs/GaSb period. Indeed, the asymmetric structure induces a reduction of SL effective masses, then a decrease of the intrinsic carrier concentration for a given temperature, leading to an improvement of R_0A product (Rodriguez et al., 2010).

5 CONCLUSIONS

Dark current measurements were performed on MWIR InAs/GaSb SL detectors with two period designs: a symmetric (10/10) and an asymmetric (8/8) SL periods. The two SL photodiodes, grown by MBE on p-type GaSb substrate, showed cut-off wavelength near 5µm at 77K. Zero-bias resistance area product R_0A equal to $3.5x10^6$ Ω.cm^2 were measured at 77K on asymmetric SL diode, one decade higher than the equivalent symmetric period design and this predominance of the asymmetric SL period structure still valid whatever the temperature operation of the diode, at low temperature when the diode is G-R limited as well as at high temperature when the diode is diffusion limited. Such results obtained demonstrate the strong importance of the selected SL period to enhance electrical performances of MWIR InAS/GaSb SL pin photodiodes. These results have to be completed by calibrated photoresponse measurements and will be the subject of forthcoming studies.

REFERENCES

Abdollahi Pour, S., Huang, E. K., Chen, G., Haddadi, A., Nguyen, B.-M, Razeghi, M., 2011. High operating temperature midwave infrared photodiodes and focal plane arrays based on type-II InAs/GaSb superlattices, *Appl. Phys. Lett.* 98, 143501.

Cervera, C., Rodriguez, J. B., Chaghi, R., Aït-Kaci, H., Christol, P., 2009. Characterization of Midwave Infrared InAs/GaSb Superlattice Photodiode, *J. Appl. Phys* 106, 024501.

Chaghi, R., Cervera, C., Aït-Kaci, H., Rodriguez J. B., Christol, P., 2009. Wet etching and chemical polishing of InAs/GaSb superlattice photodiodes, *Semicond. Sci. Technol.* 24, 065010.

Gunapala, S. D., Ting, D. Z., Hill, C. J., Nguyen, J., Soibel, A., Rafol, S.B., Keo, S. A., Mumolo, J. M., Lee, M. C., Liu, J. K., Yang, B., Liao, A., 2010. Demonstration of 1Kx1K long-wave and mid-wave superlattice infrared focal plane arrays, Proc. SPIE 7808, 780802.

Haugan, H. J., Grazulis, L., Brown, G. J., Mahalingam, K., Tomich, D. H., 2004. Exploring optimum growth for high quality InAs/GaSb type-II superlattices, *J. Cryst. Growth* 261, 471

Hood, A., Delaunay, P-Y., Hoffman, D., Nguyen, B-M. Wei, Y., Razeghi, M., 2007. Near bulk-limited R0A of long-wavelength infrared type-II InAs/GaSb superlattice photodiodes with polyimide surface passivation, *Appl. Phys. Lett.* 90, 233513.

Hill, C. J., Li, J. V., Mumolo, J. M., Gunapala, S. D., 2007. MBE grown type-II MWIR and LWIR superlattice photodiodes, Infrared Phys. Technol. 50, 187.

Kaspi, R., Steinshnider, J., Weimer, M., Moeller, C., Ongstad, A., 2001. As-soak control of the InAs-on-GaSb interface, *J. Cryst. Growth* 261, 544

Little, J. W., Svensson, S. P., Beck, W. A., Goldberg, A.C., Kennerly, S. W., Hongsmatip, T., Winn, M., Uppal P., 2007. Thin active region, type II superlattice photodiode arrays: single-pixel and focal plane array characterization, *J. Appl. Phys.* 101, 044514-6

Plis, E., Kutty, M. N., Krishna, S., 2011. Review of passivation techniques for InAs/GaSb strained layer superlattice detectors, *Laser & Photonics Reviews* 7, 1.

Rehm, R., Walther, M., Schmitz, J., Fleißner, J., Fuchs, F., Ziegler, J., Cabanski, W., 2006. InAs/GaSb superlattice focal plane arrays for high-resolution thermal imaging, *Opto-Electron. Rev.* 14, 19.

Rodriguez, J. B., Christol, P., Chevrier, F., Joullié, A., 2005. Optical characterization of symmetric InAs/GaSb superlattices for detection in the 3-5 mm spectral region, *Physica E* 28, 128.

Rodriguez, J. B., Cervera, C., Christol, P., 2010. A type-II superlattice period with a modified InAs to GaSb thickness ratio for midwavelength infrared photodiode performance improvement, *Appl. Phys. Lett.* 97, 251113.

Rogalski, A., Antoszewski, J., Faraone, L., 2009. "Third-generation infrared photodetector arrays," *J. Appl. Phys.* 105, 091101.

Satpati, B., Rodriguez, J. B., Trampert, A., Tournié, E., Joullié, A., Christol, P., 2007. Interface analysis of InAs/GaSb superlattice grown by MBE, *J. Cryst. Growth* 301, 889-892

Walther, M., Weimann, G., 2006. Infrared imaging with InAs/GaSb type-II superlattices, *Phys. Stat. sol* (a) 203, 3545.

Wei, Y., Hood, A., Yau, H., Gin, A., Razeghi, M., Tidrow, M. Z., Nathan, V., 2005. Uncooled operation of type-II InAs/GaSb superlattice photodiodes in the midwavelength infrared range, *Appl. Phys. Lett.* 86, 233106.

Yang, M. J., Bennet, B. R., 1994. InAs/GaSb infrared photovoltaic detector at 77K, *Electron. Lett*. 30, 1710-1711.